DOI 10.5012/bkcs.2011.32.5.1757

Photocatalytic Activities of Hydrothermally Synthesized Zn_2SnO_4

Myung-Jin Kim, Seong-Hun Park,† and Young-Duk Huh*

Department of Chemistry, Dankook University, Institute of Nanosensor and Biotechnology, Gyeonggi-Do 448-701, Korea
**E-mail: ydhuh@dankook.ac.kr (Y.-D. Huh)*
†Department of Chemistry, University of Seoul, Seoul 130-743, Korea
Received January 10, 2011, Accepted March 22, 2011

Key Words : Zn_2SnO_4, Hydrothermal synthesis, Photocatalytic activities

Zinc stannate (Zn_2SnO_4) is a transparent conducting oxide with high electron mobility, high electrical conductivity and low visible absorption, and is used widely as gas sensors, electrode materials, and photoluminescence materials.[1-3] Zn_2SnO_4 has also attracted considerable interest for its high photocatalytic activity. The decomposition reactions of benzene and water-soluble dyes using Zn_2SnO_4 as a photocatalyst were reported.[4-7] Zn_2SnO_4 is normally synthesized by solid state reactions with ZnO and SnO_2 at high temperatures.[8,9] The high temperature calcination of coprecipitated Zn and Sn hydroxides with the alkali from an aqueous solution were also used to prepare Zn_2SnO_4.[4,10] Recently, the hydrothermal synthesis of Zn_2SnO_4 was reported.[11-13] Hydrothermal methods have advantages over the solid state reactions and high temperature calcinations methods, such as a lower reaction temperature and simpler method for producing nano-sized particles. Therefore, hydrothermal methods should be used to prepare Zn_2SnO_4 nanoparticles to improve the photocatalytic activity. However, relatively little is known regarding the relationship between the photocatalytic activity and synthetic conditions of hydrothermal methods of Zn_2SnO_4. This paper reports the photocatalytic activity of Zn_2SnO_4 nanoparticles prepared by a simple hydrothermal method from $Zn(CH_3COO)_2$ and $SnCl_4$ with different amounts of NH_4OH to control the pH from 8 to 11. The photocatalytic activity of Zn_2SnO_4 nanoparticles prepared by hydrothermal synthesis from $Zn(CH_3COO)_2$ and $SnCl_4$ with different types of hydroxylation agents at pH 9 was also examined.

Figure 1 shows XRD patterns of the as-prepared samples obtained by hydrothermal methods from $Zn(CH_3COO)_2$ and $SnCl_4$ in the presence of different amounts of NH_4OH to control the pH from 8 to 11. At pH 8 and 9, the XRD patterns showed only a Zn_2SnO_4 phase. The products consisted of a single Zn_2SnO_4 crystals in the *Fd3m* cubic crystal system (JCPDS 24-1470, a = 0.8657 nm). When the pH was increased to 10, most of the products match the Zn_2SnO_4 phase. However, $ZnSn(OH)_6$ coexisted with Zn_2SnO_4 as minor peaks in the XRD patterns. When the pH was increased further to 11, the product consisted of a single *Pn3m* cubic crystal system of $ZnSn(OH)_6$ (JCPDS 20-1455, a = 0.7800 nm). Therefore, Zn_2SnO_4 is formed below the pH 10, and $ZnSn(OH)_6$ is formed above the pH 10.

Figure 2 shows TEM and SEM images of the Zn_2SnO_4 and $ZnSn(OH)_6$ products obtained at various pH. At pH 8 and 9, aggregated forms of Zn_2SnO_4 nanoparticles were observed, as shown in Figures 2(a) and 2(b). However, micron-sized, cubic-shaped $ZnSn(OH)_6$ products were observed at pH 11, as shown in Figure 2(d). This suggests that $ZnSn(OH)_6$ has a characteristic cubic-shaped morphology. On the other hand, Zn_2SnO_4 nanoparticles do not have a unique morphology. The coexistence of Zn_2SnO_4 and $ZnSn(OH)_6$ was observed at pH 10. Figure 2(c) shows Zn_2SnO_4 nanoparticles attached to the outer surface of the micron-sized cubic $ZnSn(OH)_6$ crystals. Figure 3 shows high-resolution TEM (HRTEM) image of the Zn_2SnO_4 nanoparticles obtained at pH 9. The size of the individual nanoparticle was approximately 10 nm. The observed lattice spacing of 0.49 nm corresponded to the (111) plane of cubic Zn_2SnO_4 crystals. The fast Fourier transform (FFT) pattern corresponds to the lattice fringe, as shown in the inset of Figure 3.

To examine the photocatalytic activity of Zn_2SnO_4 and $ZnSn(OH)_6$ products obtained by hydrothermal methods, Rh6G was chosen as the pollutant model molecule. The photodegradation of Rh6G under UV lamp irradiation after the addition of Zn_2SnO_4 and $ZnSn(OH)_6$ as photocatalysts was evaluated. Figure 4(a) shows the temporal evolution of the UV-vis spectra of Rh6G in the absence of a catalyst. The absorption peaks of Rh6G decreased slightly with the irradiation time. The concentrations of Rh6G species were calculated simply from the maximum absorption intensities at 527 nm using the Beer-Lambert law. The photodegradation

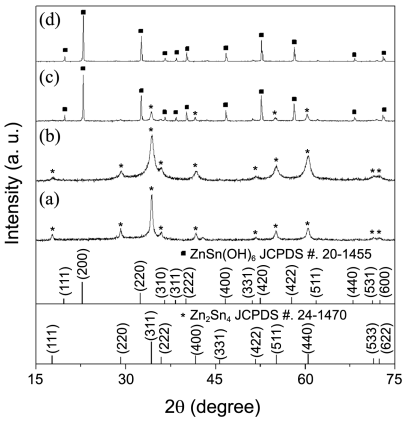

Figure 1. XRD patterns of the as-prepared samples obtained by hydrothermal methods from $Zn(CH_3COO)_2$ and $SnCl_4$ in the presence of NH_4OH at pH (a) 8, (b) 9, (c) 10, and (d) 11.

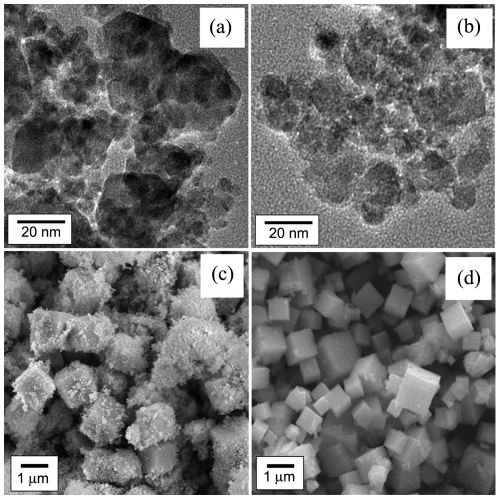

Figure 2. TEM and SEM images of the as-prepared samples obtained by hydrothermal methods from $Zn(CH_3COO)_2$ and $SnCl_4$ in the presence of NH_4OH at pH (a) 8, (b) 9, (c) 10, and (d) 11.

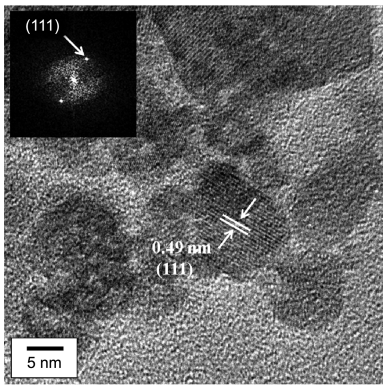

Figure 3. HRTEM image of the Zn_2SnO_4 product obtained by a hydrothermal method at pH 9. The inset shows the FFT patterns of the Zn_2SnO_4 product.

efficiency was only 2.2% for 90 min, which demonstrated that the photodegradation of Rh6G was extremely low in the absence of a catalyst. Figures 4(b), 4(c), 4(d) and 4(e) show the temporal evolution of the UV-vis spectra of Rh6G in the presence of four Zn_2SnO_4 and $ZnSn(OH)_6$ products prepared at different pH values. The absorption peaks of Rh6G decreased gradually at a given irradiation time in the presence of Zn_2SnO_4 and $ZnSn(OH)_6$. The Rh6G solution was almost decolorized after irradiation for 90 min when Zn_2SnO_4 prepared at pH 9 was used. This suggests that Rh6G was almost photodegradated within 90 min. The samples prepared at pH 8, 9, 10 and 11 have photodegradation efficiencies of 85.2%, 90.5%, 70.5% and 28.1% for 90 min, respectively. Therefore, the photocatalytic properties of Zn_2SnO_4 products were superior to those of the $ZnSn(OH)_6$ products. The Zn_2SnO_4 products prepared at pH 9 shows the highest photocatalytic property. TiO_2 powder (Degussa, P-25) was chosen as the well known reference photocatalyst to compare the photocatalytic activity of Zn_2SnO_4. Figure 4(f) shows the UV-vis spectral changes in Rh6G in the presence of TiO_2 powder. When TiO_2 powder was used, 95.1% photodegradation of Rh6G was observed after 90 min.

Most of photodegradation reactions of dyes obey first-order reaction kinetics.[14,15] The reaction rate constant can be obtained simply from the integrated form of first-order reaction kinetics according to equation (1).

$$\ln\left(\frac{C}{C_0}\right) = -kt \quad (1)$$

where C_0 is the initial concentration, C is the concentration of Rh6G after a set UV irradiation time. Figure 5 shows the first-order reaction kinetic plots of the photodegradation of Rh6G in the absence of a catalyst and in the presence of the as-prepared samples prepared at four different pH values. As shown in Figure 5, straight lines were observed. This suggests that the photodegradation of Rh6G obeys first-order reaction kinetics. The rate constant for the photodegradation of Rh6G in the absence of a catalyst and in the presence of Zn_2SnO_4 and $ZnSn(OH)_6$ products prepared at pH 8, 9, 10 and 11 were 2.0×10^{-4}, 2.0×10^{-2}, 2.5×10^{-2}, 1.4×10^{-2}, and 3.8×10^{-3} min^{-1}, respectively. Therefore, the photocatalytic activity of Zn_2SnO_4 is better than that of $ZnSn(OH)_6$. The BET surface areas of Zn_2SnO_4 and $ZnSn(OH)_6$ prepared at pH of 8, 9, 10 and 11 were 82.5, 94.8, 15.4, and 13.5 m^2/g, respectively. The photocatalytic activity of Zn_2SnO_4 depends strongly on the BET surface areas of Zn_2SnO_4. The rate constant for the photodegradation of Rh6G in the presence of TiO_2 powder was 3.1×10^{-2} min^{-1}. Based on the rate constant of photodegradation of Rh6G, the photocatalytic activity of Zn_2SnO_4 prepared at pH 9 using NH_4OH is approximately 81% that of the TiO_2 powder. $ZnSn(OH)_6$ with BET surface areas of 48 m^2/g was used as a photocatalyst for the decomposition reactions of benzene.[16] Even though overall photocatalytic activity of Zn_2SnO_4 is superior to that of $ZnSn(OH)_6$ in this work, the photocatalytic activity of $ZnSn(OH)_6$ prepared at pH 11 was slightly better than that of Zn_2SnO_4 prepared at pH 9 when rate constants are normalized to surface area. This suggest that $ZnSn(OH)_6$ with larger BET surface area can be an excellent photocatalyst. We will plan to prepare the $ZnSn(OH)_6$ with larger BET surface area to enhance the photocatalytic activitiy of $ZnSn(OH)_6$ later.

NaOH, NH_4OH, DMEDA, and TMEDA were used as a ligand and hydroxylation agent to examine the effect of the ligand on photocatalytic activity of Zn_2SnO_4 obtained using hydrothermal methods at pH 9. XRD patterns of four products matched the reported data for single Zn_2SnO_4 crystals (JCPDS 24-1470, a = 0.8657 nm) without impurities. Figure 6(a), 6(b), 6(c) and 6(d) show the UV-vis spectral changes in Rh6G in the presence of the four Zn_2SnO_4 products prepared using NaOH, NH_4OH, DMEDA, and TMEDA, respectively. The photodegradation efficiencies of Rh6G in the presence of Zn_2SnO_4 prepared using NaOH, NH_4OH, DMEDA, and TMEDA were were 74.4%, 90.5%, 95.5%, and 84.2% for 90 min, respectively. The rate constant for the photodegradation of Rh6G in the presence of Zn_2SnO_4 prepared using NaOH, NH_4OH, DMEDA, and TMEDA was 1.5×10^{-2}, 2.5×10^{-2}, 3.2×10^{-2} and 2.0×10^{-2} min^{-1}, respectively. The BET surface areas of Zn_2SnO_4

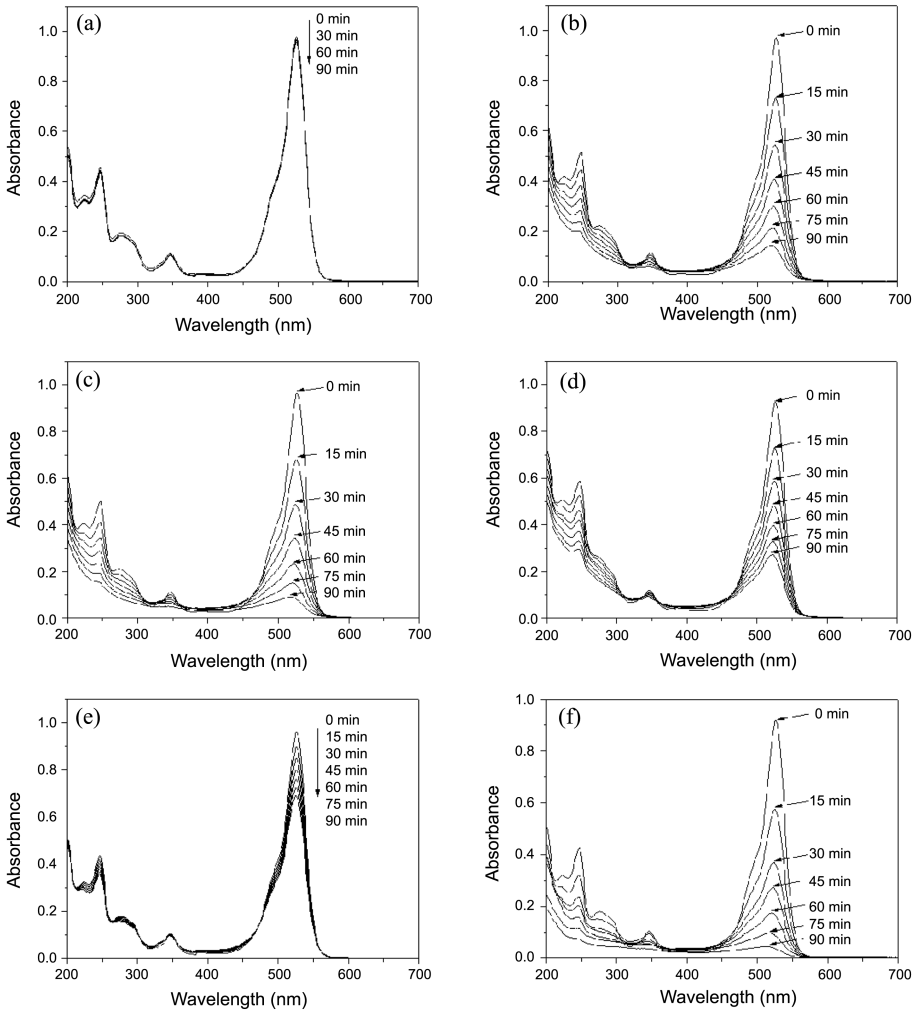

Figure 4. Absorption spectral changes in Rh6G during irradiation with UV light (λ = 254 nm) (a) in the absence of a catalyst and in the presence of the Zn_2SnO_4 and $ZnSn(OH)_6$ obtained at various pH (b) 8, (c) 9, (d) 10, (e) 11, and (f) in the presence of the TiO_2 catalyst.

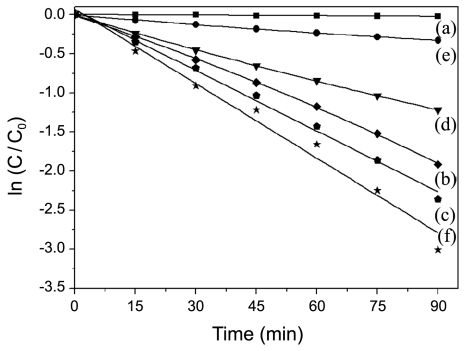

Figure 5. First-order reaction kinetic plots of the photodegradation of Rh6G (a) in the absence of a catalyst and in the presence of the Zn_2SnO_4 and $ZnSn(OH)_6$ obtained at various pH (b) 8, (c) 9, (d) 10, (e) 11, and (f) in the presence of the TiO_2 catalyst.

products prepared at pH 9 using NaOH, NH_4OH, DMEDA, and TMEDA were 57.2, 94.8, 86.6, and 61.9 m^2/g, respectively. Therefore, the photocatalytic activities of Zn_2SnO_4 products prepared at pH 9 using the different hydroxylation agents were in the following order: DMEDA > NH_4OH > TMEDA > NaOH. The photocatalytic activity of Zn_2SnO_4 prepared at pH 9 using DMEDA was approximately 103% that of the well-known TiO_2 photocatalyst.

In conclusion, Zn_2SnO_4 and $ZnSn(OH)_6$ were synthesized using a hydrothermal reaction from $Zn(CH_3COO)_2$ and $SnCl_4$ with different amounts of NH_4OH. A single phase of Zn_2SnO_4 and $ZnSn(OH)_6$ were formed at pH 8, 9, and pH 11, respectively. At pH 10, Zn_2SnO_4 and $ZnSn(OH)_6$ coexisted. The photocatalytic activity of Zn_2SnO_4 prepared at pH 9 was better than that of $ZnSn(OH)_6$ prepared at pH 11 by factor of 6.6. The photocatalytic activity of Zn_2SnO_4 nanoparticles prepared using the different hydroxylation agents were in the following order: DMEDA >NH_4OH > TMEDA > NaOH. The photocatalytic activity of Zn_2SnO_4 prepared at pH 9 using DMEDA was almost equal to that of the well-known TiO_2 photocatalyst.

Experimental Section

$Zn(CH_3COO)_2$ (98%, Aldrich), $SnCl_4$ (98%, Aldrich), NaOH (97%, Aldrich), NH_4OH (28%, Aldrich), *N,N*-dimethyl ethylenediamnie (DMEDA, 95%, Aldrich), *N,N,N′,N′*-tetramethyl ethylenediamnie (TMEDA, 99%, TCI), Rhodamine 6G (Rh6G, 99%, Aldrich), and TiO_2 powder (Degussa, P-25) were used

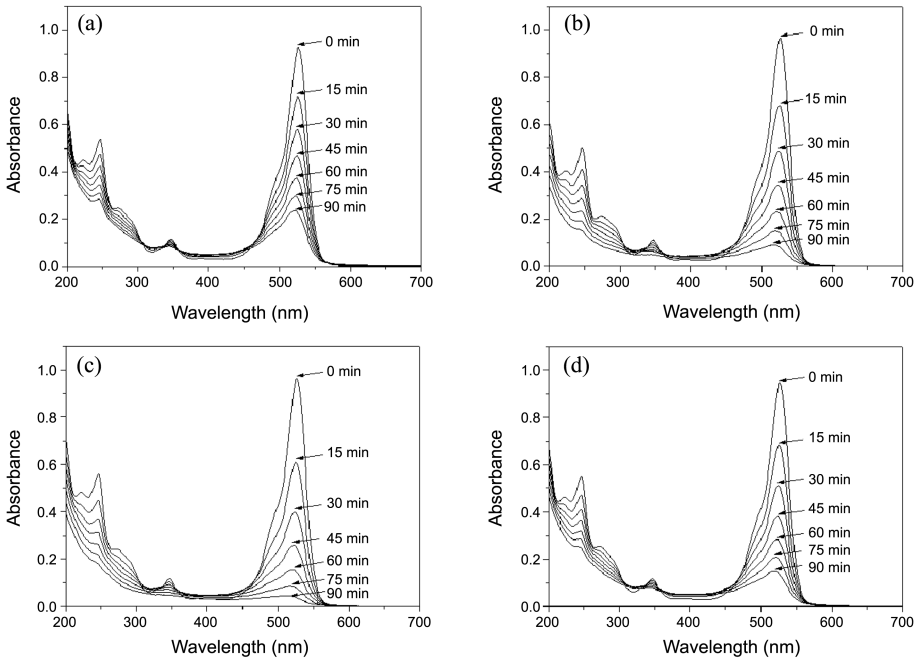

Figure 6. Absorption spectral changes in Rh6G during irradiation with UV light (λ = 254 nm) in the presence of four Zn_2SnO_4 products prepared at pH 9 using (a) NaOH, (b) NH_4OH, (c) DMEDA, and (d) TMEDA as a hydroxylation agent, respectively.

as received. In a typical experiment, 20 mL of a 0.10 M $Zn(CH_3COO)_2$ solution was added to 20 mL of a 0.05 M $SnCl_4$ solution. Different amounts of a NH_4OH solution was added to the mixed solution to obtain the various pH values (pH 8, 9, 10, and 11). A 60 mL sample of the final solution was transferred to a 100 mL Teflon-lined autoclave and heated to 140 °C for 16 h. The product was filtered, washed several times with ethanol and water, and dried at 80 °C for 12 h.

The photocatalytic activity of the Zn_2SnO_4 and $ZnSn(OH)_6$ samples was evaluated by the photodegradation of Rh6G under a 12 W UV lamp (λ = 254 nm). In a typical procedure, 10 mg Zn_2SnO_4 (or $ZnSn(OH)_6$) powder was added to 100 mL of 1.04×10^{-5} M Rh6G aqueous solutions in a 100 mL round bottom flask. The suspensions were then irradiated under a UV lamp at a 3 cm separation distance in dark condition. Every 15 minutes during the photodegradation process, 3 mL of the Rh6G solution was sampled and separated by centrifugation. The concentrations of the supernatants were monitored using a UV-vis spectrophotometer. To compare the photocatalytic activitiy of TiO_2 with that of Zn_2SnO_4, 10 mg of TiO_2 was used with the other conditions kept the same as those used for the photodegradation of Rh6G by adding Zn_2SnO_4.

The structures of the Zn_2SnO_4 and $ZnSn(OH)_6$ products were characterized by powder X-ray diffraction (XRD, PANalytical, X'pert-pro MPD) using Cu Kα radiation. The morphology of the products was observed by scanning electron microscopy (SEM, Hitachi S-4300) and transmission electron microscopy (TEM, JEOL JEM-3010). The Brunauer-Emmett-Teller (BET) surface areas of the sample were calculated from the N_2 adsorption/desorption isotherms determined at liquid nitrogen temperature using an automatic analyzer (Micrometric, Tristar 3020). Prior to adsorption, the samples were outgassed for 8 h under a vacuum at 120 °C.

Acknowledgments. This study was supported by Basic Science Research Program through National Research Foundation of Korea funded by the Ministry of Education, Science and Technology (2010-0007492).

References

1. Yamada, Y.; Seno, Y.; Masuoka, Y.; Yamashita, K. *Sens. Actuators B* **1998**, *49*, 248.
2. Tan, B.; Toman, E.; Li, Y.; Wu, Y. *J. Am. Chem. Soc.* **2007**, *129*, 4162.
3. Wang, J. X.; Xie, S. S.; Yuan, H. J.; Yan, X. Q.; Liu, D. F.; Gao, Y.; Zhou, Z. P.; Song, L.; Liu, L. F.; Zhao, X. W.; Dou, X. Y.; Zhou, W. Y.; Wang, G. *Solid State Commun.* **2004**, *131*, 435.
4. Cun, W.; Xinming, W.; Jincai, Z.; Bixian, M.; Guoying, S.; Ping'an, P.; Jiamo, F. *J. Mater. Sci.* **2002**, *37*, 2989.
5. Foletto, E. L.; Jahn, S. L.; Moreira, R. F. P. M. *J. Appl. Electrochem.* **2010**, *40*, 59.
6. Lou, X.; Jia, X.; Xu, J.; Liu, S.; Gao, Q. *Mat. Sci. Eng. A* **2006**, *432*, 221.
7. Fu, X.; Wang, X.; Long J.; Ding, Z.; Yan, T. Zhang, G.; Zhang, Z.; Lin, H.; Fu, X. *J. Solid State Chem.* **2009**, *182*, 517.
8. Jie, J.; Wang, G.; Han, X.; Fang, J.; Yu, Q.; Liao, Y.; Xu, B.; Wang, Q.; Hou, J. G. *J. Phys. Chem. B* **2004**, *108*, 8249.
9. Chen, H.; Wang, J.; Yu, H.; Yang, H.; Xie, S.; Li, J. *J. Phys. Chem. B* **2005**, *109*, 2573.
10. Wang, S.; Yang, Z.; Lu, M.; Zhou, Y.; Zhou, G.; Qiu, Z.; Wang, S.; Zhang, H.; Zhang, A. *Mater. Lett.* **2007**, *61*, 3005.
11. Zhu, H.; Yang, D.; Yu, G.; Zhang, H.; Jin, D.; Yao, K. *J. Phys. Chem. B* **2006**, *110*, 7631.
12. Alpuche-Aviles, M. A.; Wu, Y. *J. Am. Chem. Soc.* **2009**, *131*, 3216.
13. Zeng, J.; Xin, M. D.; Li, K. W.; Wang, H.; Yan, H.; Zhang. W. J. *J. Phys. Chem. C* **2008**, *112*, 4159.
14. Lin, J.; Lin, J.; Zhu, Y. *Inorg. Chem.* **2007**, *46*, 8378.
15. Kim, M. J.; Huh, Y. D. *Mater. Res. Bull.* **2010**, *45*, 1921.
16. Fu, X.; Wang, X.; Ding, Z.; Leung, D. Y. C.; Zhang, Z.; Long, J.; Zhang, W.; Li, Z.; Fu, X. *Appl. Catal. B* **2009**, *91*, 67.